

Vitrification in a 2D Ising model with mobile bonds

Predrag Lazić and D. K. Sunko,*

Department of Physics,

Faculty of Science,

University of Zagreb,

Bijenička cesta 32,

HR-10000 Zagreb, Croatia.

Abstract

A bond-disordered two-dimensional Ising model is used to simulate Kauzmann's mechanism of vitrification in liquids, by a Glauber Monte Carlo simulation. The rearrangement of configurations is achieved by allowing impurity bonds to hop to nearest neighbors at the same rate as the spins flip. For slow cooling, the theoretical minimum energy configuration is approached, characterized by an amorphous distribution of locally optimally arranged impurity bonds. Rapid cooling to low temperatures regularly finds bond configurations of higher energy, which are both *a priori* rare and severely restrictive to spin movement, providing a simple realization of kinetic vitrification. A supercooled liquid regime is also found, and characterized by a change in sign of the field derivative of the spin-glass susceptibility at a finite temperature.

1 Introduction

In a seminal article many years ago, Kauzmann [1] provided the now standard [2] physical picture of vitrification in liquids, which emphasized that

*email: dks@phy.hr

obstruction of configurational rearrangement by molecular interactions could lead to such an inefficient sampling of phase space, that thermodynamic equilibrium could not be reached for very long times. The ability to change configuration practically disappears at the glass transition, while orientational disorder does not change significantly, being high and relatively static in both the supercooled liquid and the glass. For our simple purposes, the scenario may be compared to a log-jam. There is nothing in the Hamiltonian to prevent orderly stacking, and indeed, vitreous liquids possess a crystal state of lower free energy. But once the logs are jammed, it is (very) improbable they will be ordered by random pushing and pulling.

By contrast, in spin glasses [3, 4], the Hamiltonian itself forbids crystal order, because of impurities, or lattice topology. Now disorder in terms of the original microscopic variables becomes an equilibrium property at all temperatures, leaving open the possibility of a true thermodynamic phase transition in terms of some other, less-than-obvious order parameter. In searching for it, the basic concept is frustration, introduced [5] to distinguish ‘intrinsically’ disordered states from those where apparent disorder can in fact be removed by redefining parameters of the Hamiltonian. These ‘serious’ and ‘trivial’ kinds of disorder may be called respectively ‘glassy’ and ‘amorphous’.

In the present article, we bring the two subjects together, to obtain a toy model of kinetic vitrification. In brief, our algorithm gives a structural glass in a spin-glass setting. We begin with the discrete bond-disordered Ising model in two dimensions. It is known [6] that it has no spin-glass transition at $T > 0$. Topologically frustrated configurations are too rare in two dimensions to contribute significantly to the sample-averaged free energy, when each random arrangement of impurities contributes a sample with equal *a priori* probability. We refer to this standard quenched-disorder picture as ‘frozen’ or ‘frozen bonds’, reserving the word ‘quenched’ as follows.

The model we consider is obtained from the above by allowing the impurity bonds to move. Throughout the article, ‘quenching’ means that this system, with movable bonds, is first equilibrated at high temperature, and the temperature then brought down to some low value in a single step, after which the evolution continues at that low temperature. Since the bonds move, there is no averaging over samples; the complete impurity configuration space is available to a single sample. Of course, the efficiency with which this space is explored after the quench critically depends on the nature of bond movement. We focus on the case where they move locally, *i.e.* a bond can only exchange places with another bond, impinging on the same site.

Our main point is that such an algorithm, which would be very inconvenient to study the ground state of the disordered Ising model, because it is easily trapped in metastable states, is very convenient from the structural-glass point of view, because the metastable states in which it does get trapped are quite exceptional among all possible impurity arrangements, and are analogous to vitreous states in the structural sense.

It is easy to imagine how this happens: the bonds keep moving until they get stuck. These ‘stuck’ configurations are precisely the vitreous ones, which are (by definition) those in which evolution ceases before the ground state is reached. Various signals of their exceptional nature are studied throughout the article; let us only mention that their energy is markedly lower than the average energy in the frozen scenario, in fact close to the theoretical ground state energy (which can also be reached, by slow cooling). Nevertheless, it is finitely above the ground state, making them (by definition) metastable.

In the present work, we consider only the fast evolution after a quench, leading to the above-mentioned metastable states, and the evolution of these states at intermediate times, but not their relaxation to the ground state, occurring at much longer time scales. The ground state (annealed system) is a comparatively trivial amorphous configuration, and our only interest in it is that it establishes the formal metastability of the long-lived quenched states. In this, of course, our toy model is different from a true vitreous liquid, where the ground state is an ordered crystal. The model analogue of melting involves no order-disorder transition.

In the description of our results, we use established language (*e.g.*, melting) and theoretical tools (*e.g.*, the spin-glass susceptibility) somewhat outside their original context. The model is purely kinetic, without a thermodynamic phase transition, so the term ‘equilibrium’ refers in fact to the quasi-equilibrium, established at the above-mentioned intermediate time scale. We are guided by an intuitive analogy between spins and bonds in the disordered Ising model, on the one side, and the orientational and configurational degrees of freedom, respectively, of a glass-former, on the other.

One class of Ising-like models, often used to study vitrification, are constrained kinetics models, such as the Frederickson-Andersen model [7]. They have no intrinsic disorder, but frustration is introduced by dynamical restrictions on changing the spin states, which take the part of configurational variables. Among work on variants of the disordered Ising model, our program is closest to that of the frustrated percolation problem [8, 9]. However, that approach views impurity bonds as obstacles to rearrangement, playing

a role similar to the dynamical restrictions, mentioned above. In our work, bonds are imagined to represent the configurational degree of freedom itself, so their movement becomes of physical interest. It is responsible for the appearance of metastable states, the ‘supercooled bond liquid’, which have a distinct physical characteristic, a first-order zero in the field derivative of the spin glass susceptibility, not shared by the states on the cooling curve connected to the ground-state manifold. This liquid, and the accompanying glass, are the main subject of the present article.

2 Model and algorithm

The model is the bond-disordered two-dimensional Ising model on a square lattice [12]:

$$H = - \sum_{\langle ij \rangle} J_{ij} S_i S_j - B \sum_i S_i \equiv - \sum_{\langle ij \rangle} J_{ij} S_i S_j - B \cdot M, \quad (1)$$

where the ‘spins’ take the values $S_i = \pm 1$, as well the bonds, $J_{ij} = \pm 1$. Here M is the total magnetization, calculated as above, not an independent parameter. The fraction of antiferromagnetic (negative J_{ij}) bonds is a fixed number p ; in this paper, $p = 70\%$. The key new feature is the ability of bonds to move; this is considered to be purely diffusive, so there is no kinetic contribution to the Hamiltonian.

Spin updates proceed by flipping a spin at random; the criterion for acceptance is Glauber’s. Between spin updates are bond updates; the test move is to exchange two bonds of the opposite sign, impinging on the same site. This is accepted or rejected, again by the Glauber criterion. Which bonds are exchanged, and on which site, is chosen at random, taking care, of course, that the two bonds involved are indeed of the opposite sign. There is no regular ‘sweeping’ of the lattice, to avoid artificial correlations between spin and bond updates.

There still remains a physical freedom in the update protocol. One might consider, in general, flipping s spins and moving b bonds, before submitting the new configuration for acceptance. These are large steps in the random-walker picture. They are unlikely to be accepted in general, but once the system is trapped in a glassy state, such steps may significantly affect its chance to get out. These rare ‘cooperative’ fluctuations are considered responsible for re-crystallization of vitreous liquids in the Kauzmann picture, sometimes after ‘archeologically’ long times, as in window glass.

In this work, we only focus on driving the system into a glassy state, not getting it out. On this ‘laboratory’ time scale, alternating one-spin and one-bond updates, each subject to acceptance in turn, provide the dominant quasi-equilibration mechanism. The very-long-time behavior of the model is the subject of a limited investigation in Section 4 below, but still neglecting multistep (cooperative) processes, which could be important for the asymptotic regime. Parenthetically, we note that mode-coupling theory introduces an artificial thermodynamic transition, and therefore certainly has the wrong asymptotics, but even this does not affect the intermediate time scales, for which it was devised [10].

We consider two situations: annealed, where the system is equilibrated at high temperature ($T = 5$, but any $T > 2$ will do), and then slowly cooled (in steps of 0.05, waiting to equilibrate between temperature steps); and quenched, where it is brought down to the desired temperature in a single step from the high-temperature equilibrium, and then (quasi)equilibrated. The high-temperature starting point is generated anew for each quenched point, so the agreement of annealed and quenched curves for not-too-low temperatures is also a check of equilibration. Similarly, the fact, that the annealed curve nearly reaches the ideal (defect-free) ground state energy at $T = 0.05$, our lowest temperature, is indication that the cooling rate for annealment ($\Delta T \sim 10^{-9}$ per MC step) is sufficiently slow for our purposes.

For comparison, we shall also simulate some systems with frozen bonds. This opens the question of sample-averaging. We find that self-averaging is sufficient for our limited purpose, since the samples involved are rather large (100×100 and larger). To be safe, we have made some runs, averaging batches of up to 500 small ($\sim 10 \times 10$) samples, and indeed no claims made in the paper, based on the large self-averaged ones, were affected. Note, also, that the frozen bond arrangement at high temperature is different for each cooling run, so the above-mentioned check of equilibration is also a check of self-averaging in the frozen case.

3 Main result

All simulations were performed in a uniform external field, whose non-trivial range is $0 \leq B \leq 4$. Then the theoretical minimum energy per site of the annealed system with a fraction p of antiferromagnetic bonds is

$$U_{\min} = -2 - (1 - p)B, \quad (2)$$

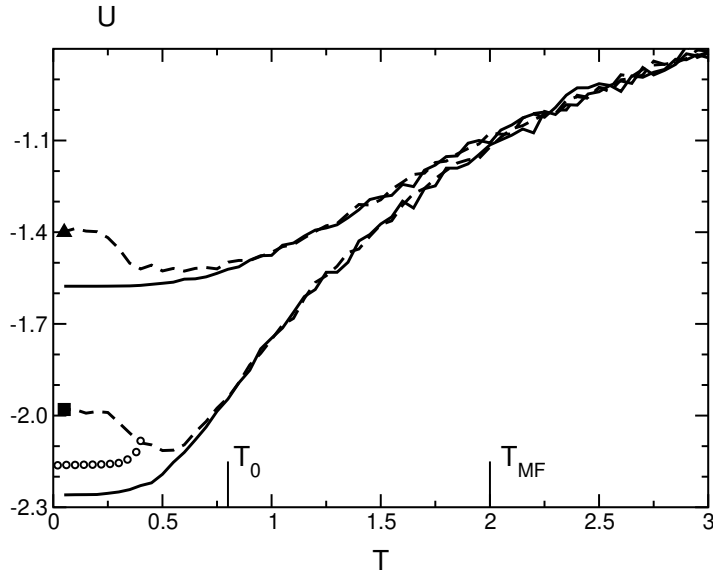


Figure 1: Energy per site for $p = 0.7$ and $B = 1$. Full curves: annealed. Dashed curves: suddenly cooled. Lower (upper) two curves: with (without) bond movement. Open circles: quench to $T = 0.4$ and slow cooling. Symbols at $T = 0.05$: see Figs. 2 and 3. $U_{\min} = -2.3$ [Eq. (2)], lattice 100×100 .

which assumes the absence of defects: each spin, turned opposite to the field, is connected to its neighboring sites by antiferromagnetic bonds, which are all used up in this way. These ‘crosses’ carry no frustration, obviously: a simultaneous sign change of the spin and its four bonds leads to a perfect ferromagnet. There is a ground-state entropy, associated with their random placing on the lattice, so this ideal state is amorphous. It is our model’s analogue of the crystal state of vitreous liquids.

A convenient robust measure of additional disorder is the energy mismatch between this reference state and one obtained in an actual run. This can be extended to any temperature by using the reference system’s cooling curves, once it is checked that its zero-temperature limit is near the theoretical amorphous one, *i.e.*, that it is sufficiently annealed.

Figure 1 shows the energies per site for a single cooling run, in an external field $B = 1$ and $p = 0.7$. Four curves are given, annealed and suddenly cooled, with and without bond movement allowed. Two energy scales appear: a higher one, where the curves with bond movement separate, and a lower one, distinguishing annealed and suddenly cooled systems. Unexpectedly,

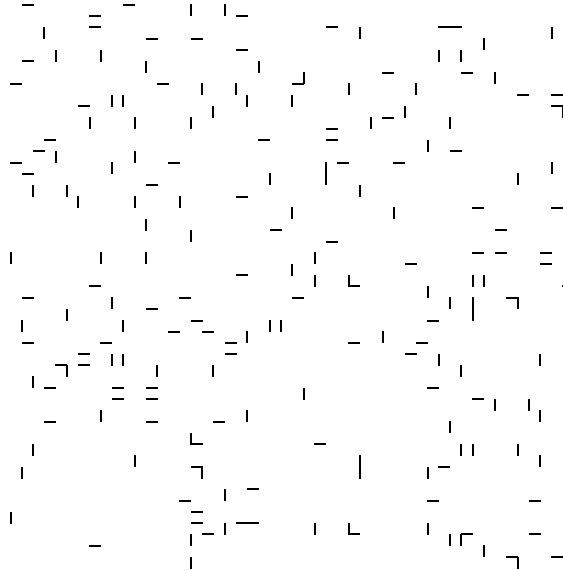


Figure 2: A 50×50 segment of the quenched state, marked by a filled square in Fig. 1. Only uncompensated bonds are shown. The preponderance of singletons indicates nearly all the disorder is glassy.

the higher scale is about the square root of the coordination, which is the mean-field transition temperature of the model (1), $T_{MF} = \sqrt{z} = 2$; this may be a coincidence. The lower one, denoted T_0 , is the model's melting temperature, a notion made precise in section 4.1 below. The main interest in this work is the range beneath it.

Below T_0 , the dashed curves rise with falling temperature, because each point on them is generated anew by a drop from high temperature. The lower the temperature to which they are quenched, the ‘worse’ (energetically) the state in which they end. In the next section, we shall discuss a third type of cooling run, where the system is cooled slowly after a quench from high temperature. An example of this is also given in the figure, showing the thermodynamically expected behavior.

While the two dashed curves look similar, they refer to very different states. In Figures 2 and 3, we draw the respective lattices at low temperature, presenting only uncompensated bonds, *i.e.* those which are of the ‘wrong’ sign relative to the spins they connect. The exact ground states have as few of these as possible (a nonzero number may be topologically unavoidable [11]). The quenched state obviously has more, but the point is that

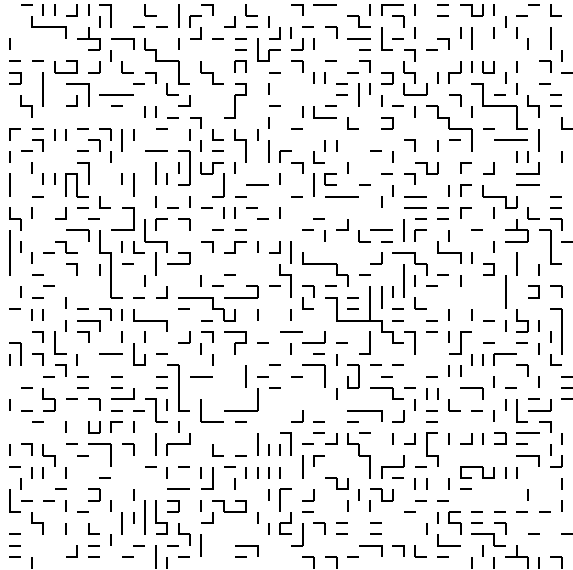


Figure 3: A 50×50 segment of the frozen, rapidly cooled state, marked by a filled triangle in Fig. 1. Only uncompensated bonds are shown. Much of the disorder is amorphous.

they nearly always appear as well-separated singletons, carrying topological frustration. In other words, the frustration of our vitreous states is near the maximal possible one, for a given energy difference from the ground state. In consequence, spin orientation is fixed by a ‘majority vote’ of bonds *at every single site* (almost). The comparatively small energy difference between the ground and vitreous states is misleading; the two are separated by a topological barrier. The fact that such *a priori* rare states can be generated with so little effort, about 50 updates per site, is an important practical point of this work.

By contrast, in the case with frozen bonds, there appear many sites with two compensated and two uncompensated bonds, making the spin orientation energetically indifferent. Many of the corresponding plaquettes are not frustrated, so the energy difference relative to the ground state is largely due to trivial (amorphous) disorder. Because of this, the magnetization of the frozen-bond system is a sum of fluctuating contributions even at low temperature, making it constant in time only on the average, while the magnetization of the vitreous (quenched) system is a sum of spins which are individually fixed in time for the lifetime of the glass, as would be the case for all times

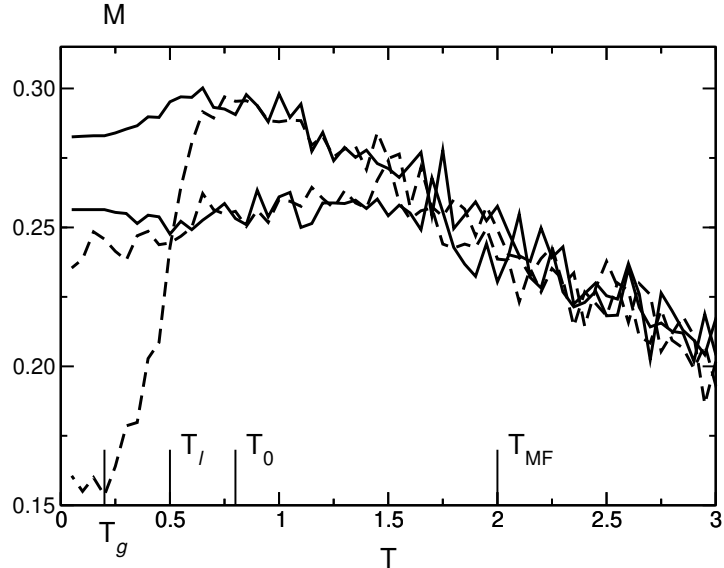


Figure 4: Magnetization per site for $p = 0.7$ and $B = 1$. Full curves: annealed. Dashed curves: quenched. Middle two curves: frozen bonds. The other two curves: mobile bonds. $M_{\max} = 0.3$ [Eq. (2)], lattice 100×100 .

with a perfect Ising ferromagnet at sufficiently low temperature.

Figure 4 shows the magnetization. For a frozen bond configuration, it barely distinguishes between annealing and quenching. What is unexpected is the difference between the annealed and quenched magnetizations, when bond movement is allowed. The annealed magnetization at $T \approx 0$ is higher than when bonds are frozen, reasonably enough. The quenched one, however, is much lower, indicating a system in which spin orientation is controlled by an internal field. It is very sensitive to the T_0 scale of Fig. 1, while the same scale is hardly visible in the other three curves.

It remains to show that the state quenched (in our sense, with mobile bonds) below $T_g \approx 0.2$ fulfills the criterion for a spin glass. We call it a ‘bond glass’, to emphasize the role of bond kinetics in its formation; it is not in thermodynamic equilibrium. The transition region $T_g \approx 0.2 < T < 0.8 \approx T_0$ in Figure 4 is then a ‘supercooled bond liquid’, characterized by a scale $T_l \approx 0.5$. For temperatures above T_0 , we have a bond liquid. Carefull cooling below the melting temperature T_0 leads to the amorphous solid, described above. (Note the small downturn below T_0 in the slowly cooled curve, which seemed headed towards the theoretical maximum magnetization $M = 0.3$. It

is due to defects in the amorphous structure. The unavoidability of these is the subject of bond-percolation studies [11].)

We consider the spin-glass susceptibility, which is a time-asymptotic four-spin correlation function [4, 6]:

$$\chi_{SG} = V \int_{-1}^1 q^2 P(q) dq, \quad (3)$$

where the ‘volume’ V is the number of spins in the lattice, and $P(q)$ is the distribution of the quantity

$$Q = \lim_{\tau \rightarrow \infty} \frac{1}{\Delta\tau} \sum_{t=1}^{\Delta\tau} \left[\frac{1}{V} \sum_{i=1}^V S_i^{(1)}(\tau + t) S_i^{(2)}(\tau + t) \right], \quad (4)$$

where the superscripts on the spins denote two copies of the system, independently evolved, and ‘infinity’ is some intermediate time scale, before ergodicity is re-established, as discussed in section 4.1 below. For each temperature, we first equilibrate the system, as to produce a point in the first two figures, then make two copies of the lattice, identical in both spins and bonds, so an artificial divergence is introduced in χ_{SG} at $\tau = t = 0$. This is allowed to decay by evolving the copies independently for a further $\tau = 5 \times 10^6$ MC steps, each consisting of a spin and a bond trial, or only a spin trial, for the cases with frozen bonds. The distribution $P(q)$ is obtained by considering the next $\Delta\tau = 2.2 \times 10^6$ steps.

In the frozen case, this is done differently [6]: one randomizes the spins in both copies of the lattice, with the *same* bond arrangement, and waits for the correlation function to build itself up again from zero. We cannot do that, because the bonds also move: once the spins are randomized, bonds start flowing, and the lattice copies end up as distinct samples, as soon as the vitreous state is re-established, which takes a very short ‘ β -relaxation’ time, only ~ 50 updates per site in our algorithm. In the usual picture of a glass free energy landscape, the two copies end in distinct deep and narrow minima, and the scale associated with tunneling between such minima is the long ‘ α -relaxation’ time. In the same language, the time window $\Delta\tau$, used above, is opened after ~ 20 times the β -relaxation period, *i.e.* in the quasi-equilibrated regime, $\tau_\beta < t < \tau_\alpha$ for all T , which is the regime of interest here.

The use of the spin-glass susceptibility should not be construed to mean, that there is a true thermodynamic transition in the model. As long as the

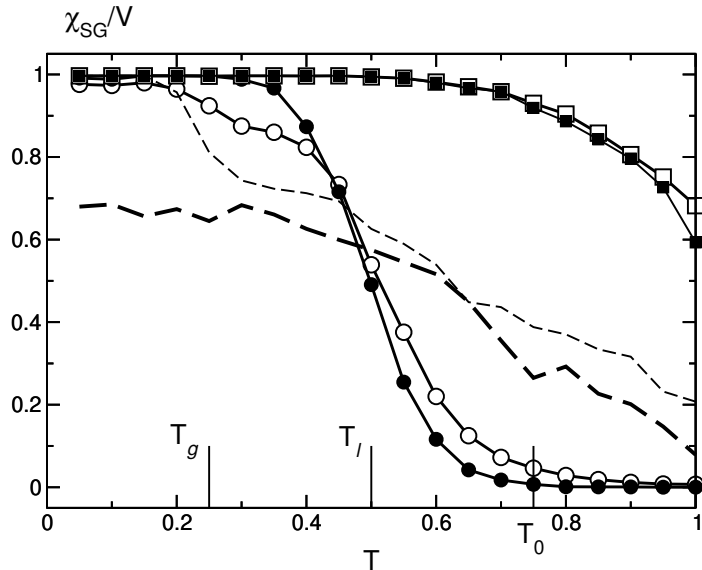


Figure 5: Normalized spin-glass susceptibility on a 120×120 lattice, for a number of quenching scenarios. Empty symbols: $B = 1$. Filled symbols: $B = 0^+$. Circles: quench with movable bonds. Squares: same as circles, but no bond movement after $\tau = t = 0$. Thick (thin) dashed line: $B = 0^+$ ($B = 1$), random frozen bonds. Zero-field T_g , T_l and T_0 are also given.

bonds move, all the reported phenomena are kinetic in origin. Asymptotically, χ_{SG} is zero at all temperatures, but the time needed to see this increases exponentially with falling temperature, as discussed in the next section.

The results are shown in Figure 5, which we discuss for the remainder of this section. The open circles correspond to the quenched bonds in Figure 4. The range $T < 0.2$, where the magnetization saturates at $M \approx 0.15$, is clearly linked to a divergence in χ_{SG} . The crossover region, $0.2 < T < 0.8$, is also evident in both figures.

The thin dashed line corresponds to the frozen-bond scenario, whose magnetization is the nearly horizontal dashed line in Figure 4. It saturates at $\chi_{SG}/V = 1$ as well, which may cause doubt about the alleged special nature of the state, found by bond movement. To dispel it, we repeat all of the above with the magnetic field turned off. (We put $B = 0.001$ to break inversion symmetry, and denote this $B = 0^+$.) The frozen-bond susceptibility then drops to the lower, thick dashed curve, which no longer shows saturation.

tion. This indicates its divergence at finite field was in fact trivial, due to the difficulty of flipping spins when $T \ll B$, so the spins on the two copies ‘marched together’ for a long time.

The quenched susceptibility shows precisely the opposite behavior, given by the filled circles. For $B = 0^+$ it rises above the $B = 1$ points, to achieve nearly perfect divergence for $T < 0.3$, but drops below them in the high-temperature part, so the net effect is a narrower crossover (supercooled liquid) region, $T_g = 0.25 < T < 0.75 = T_0$, its center (half-point of χ_{SG}/V) remaining at $T_\ell = 0.5$. The low-temperature divergence in the quenched case is due to the bonds ‘holding’ the spins, in place of any external field. The field *widens* the supercooled liquid regime, and produces a less perfect glass (slightly smaller χ_{SG} below $T = 0.2$). At $B = 0^+$ nothing is visible in the magnetization, which fluctuates around zero at all temperatures.

We now turn to the role of bond rearrangement in the supercooled liquid. We restart the evolution from the same copies of the lattice as gave the circles in Figure 5, but now disallow further bond movement. In other words, we proceed as with frozen bonds (the dashed curves), but for the special bond configurations found by quenching, not random ones. Then the open and filled circles go over into the respective squares. The supercooled liquid has disappeared, replaced by a glass up to $T \approx T_\ell$. This is in accord with the idea, that changing configurations is essential for the liquid. It may appear that the crossover has merely moved to higher temperatures, not shown in the figure. But $T = 0.8$ is already the melting temperature in Figure 4, so the system cannot be ‘supercooled’ at $T > T_0$. It melts, as it eventually must, by a trivial high-temperature degradation of the initial spin orientations. However, the rarity of the bond configurations involved is evident in the lack of field-dependence of the susceptibility (the squares nearly overlap), in sharp contrast with the behavior of the dashed curves.

4 Equilibration

The basic point of this article is that the algorithm with bond movement is physically interesting in itself, as a model realization of a structural glass. At present, we have no physical argument that the degrees of freedom of any particular real glass map onto our model. So one has at best an analogy, or ‘toy model’, and the idea is to use the analogy to guide model investigations. Some quantitative evidence will be presented in this section, that the

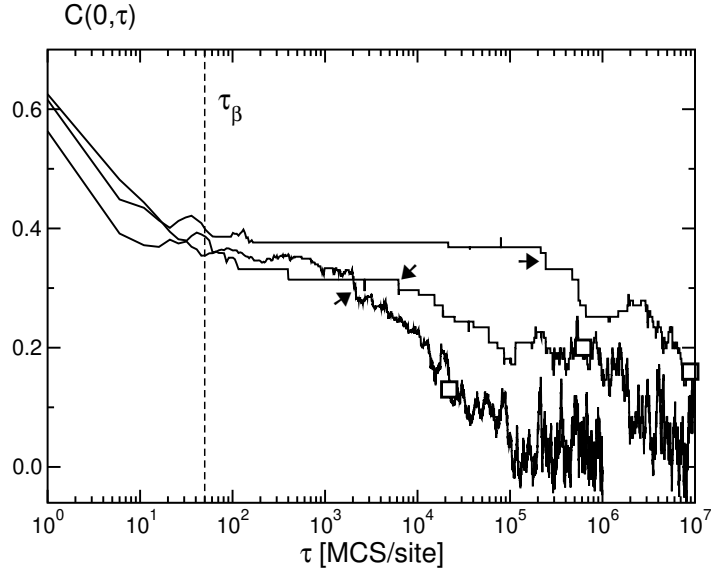


Figure 6: Spin autocorrelation function, quenched case, high-temperature initial state. Left to right by arrows: $T = 0.4$ ($L = 25$), $T = 0.3$ ($L = 15$), $T = 0.25$ ($L = 15$). Arrows: dip marking $\tau_{\alpha 1}$. White squares: points with abscissa given by Eq. (6). Dashed line: a minimal τ_{β} , for all cases.

properties uncovered in this way are not spurious.

4.1 Short and long times

In Figure 6, we show the spin autocorrelation function

$$C(t, \tau) = \frac{1}{V} \sum_{i=1}^V \langle S_i(t) S_i(t + \tau) \rangle, \quad (5)$$

where the brackets denote an average over time-windows of 10 MCS/site. The reference state ($t = 0$) is taken to be the high-temperature equilibrium ($T = 5$) before the quench. A typical two-time evolution is observed. After a short β -equilibration time τ_{β} , 50–100 MCS/site, the system enters a long-lived low-temperature state. This intermediate period, in which evolution almost seems to stop, ends at a time $\tau_{\alpha 1}$, when $C(0, \tau)$ begins to decay further, reaching zero only after a much longer time $\tau_{\alpha 2}$. The latter is usually called τ_{α} , at which time ergodicity is re-established. This is the time needed

to tunnel between the ‘deep and narrow’ minima characterizing the glass free energy landscape. In the same picture, $\tau_{\alpha 1}$ would be the time needed to exit the original minimum, which trapped the system at $t \approx \tau_{\beta}$.

It is easy to estimate $\tau_{\alpha 2}$ in the present model, because Fig. 2 indicates maximal topological frustration is a reasonable hypothesis. This implies, roughly, that *each* spin needs to flip against the local field before the state is completely dissolved. In other words, the reciprocal probability for a single spin to flip is the waiting time for dissolution, measured in updates per site. The energy difference for a flip is $\Delta E = 4$ or $\Delta E = 8$, depending on whether the spin is held in place by three or four compensated bonds. Taking the lesser of these gives an underestimate,

$$\exp\left(\frac{4}{T}\right) < \tau_{\alpha 2} \text{ [MCS/site]}, \quad (6)$$

which we find to be logarithmically correct (Fig. 6). It predicts $\tau_{\alpha 2} > 5 \times 10^{34}$ updates per site at $T = 0.05$.

The success of the simple estimate (6) indicates that the algorithm with nearest-neighbor bond diffusion realizes, more or less, the maximal time scales possible in the model, for a purely kinetic scenario. But it also implies that the scenario is indeed kinetic: nothing really happens at T_g , except that a time scale becomes too long to follow. This is the reason the present approach is computationally so cheap. One knows in advance that, say, χ_{SG} in Fig. 5 is asymptotically zero. The question is, for what delay [τ in Eq. (4)] it is most informative of the processes in the system. This turns out to be fairly modest, $\sim 10^3$ updates per site. By then, the value of T_g is as well established as for 10^6 updates, while the τ_{α} for most of the higher temperatures are still not reached, giving the largest possible range in temperature, for which $0 < \chi_{SG} < 1$. Of course, there is a highest temperature, where $\tau_{\alpha 2} \rightarrow \tau_{\beta} \approx 50$. This is just the melting temperature T_0 : $\exp(4/T_0) \approx 50$ gives $T_0 \approx 1$, as found in Fig. 1. Above it, χ_{SG} is zero at all times.

4.2 Aging

After the initial relaxation has passed, the supercooled liquid/glass spends a long time in a state which is nominally metastable, since its energy is above that of the annealed state (Fig. 1). However, it is equilibrated from the point of view of correlations; there is no ‘aging’ [13] in the metastable state. In such a quasi-equilibrium, the autocorrelation function (5) does not

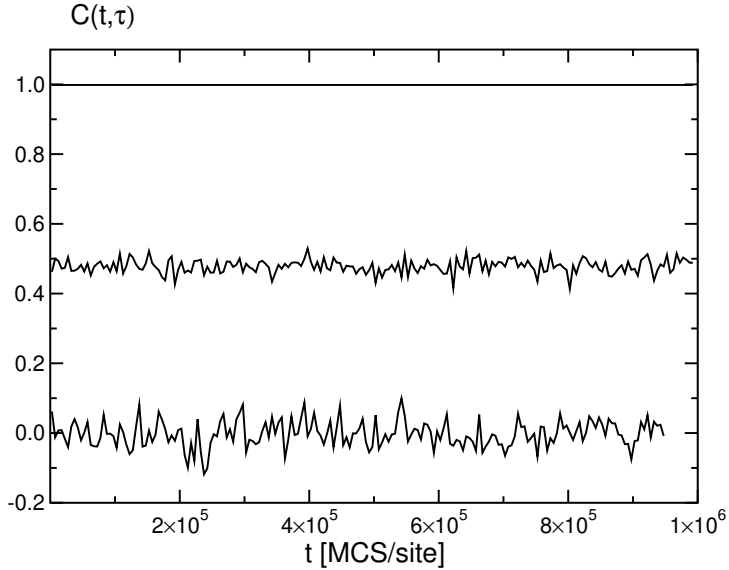


Figure 7: Spin autocorrelation function, quenched case, for $t > \tau_\beta$. Bottom to top: 1) $T = 0.6$, $L = 25$, $\tau = 10^5$ MCS/site; 2) $T = 0.6$, $L = 15$, $\tau = 10^3$ MCS/site; 3) $T = 0.2$, both cases. Time-averaging is over 10^4 updates per site.

depend on choice of origin t , apart from noise, as shown in Figure 7. Here all $t > \tau_\beta$, so the initial (reference) state is always a quasi-equilibrated one. The amplitude of the noise generally increases with τ and the temperature, while it decreases as the system gets larger. At $T = 0.2$, $C(t, \tau) = 1$, and there is no noise, for the trivial reason, that the state below T_g does not evolve at the scale of the waiting times exhibited here.

4.3 Rattling and relaxation

It is illustrative of the qualitative behavior of the model, to look at the acceptance rates of various kinds of trial moves. They are the inverses of the time scales involved. We introduce a third type of cooling run, most similar to a real experiment. In zero field, the system is first quenched into the supercooled region (below T_0), and then slowly cooled through T_g , in steps of 0.02. We look at the time evolution leading to equilibration (not after it, as in the study of χ_{SG}). After the temperature is brought to the desired value, a 120×120 lattice is subject to 7.2×10^6 spin trials, interlaced with the

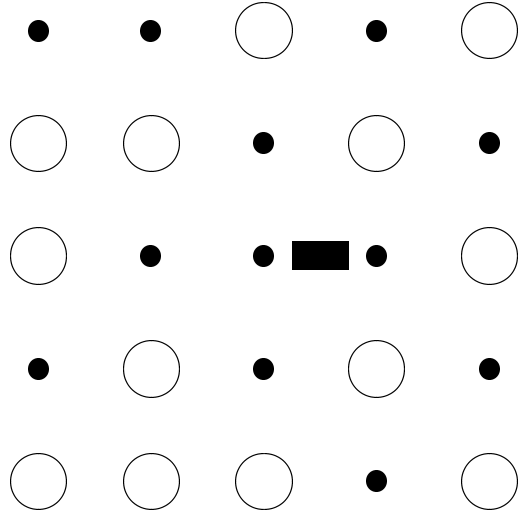


Figure 8: A ‘caged’ AF bond, free to rotate around the central spin. The other bonds (not shown) are all of the correct sign, corresponding to the spins they connect. This bond could be freed by flipping any of the four spins in the centers of the square sides, except the right-hand one.

same number of bond trials. The principal quantity monitored is the number of accepted relaxation steps, *i.e.* those in which the energy changes either way (positive changes are counted as relaxation, because they also mean the system is ‘working’).

The estimate (6) indicates that by lowering the temperature below T_g , one can really prevent the system from reaching the annealed state, in any fixed time. In addition to the disappearance of spin flips, the nature of bond movement changes below T_g , and only ‘rattling’ [2] of the kind depicted in Figure 8 survives. For our purposes, we do not define ‘rattling’ geometrically, but by the property that the move is energetically indifferent, so that it cannot contribute to annealing, by definition.

In Figure 9, we show the total number of relaxation steps, accepted during the run above. Bond relaxation disappears around T_g , while spin relaxation stops earlier, and is a rough order of magnitude less significant everywhere. Spin rattling vanishes along with bond relaxation. Thus both the energy and magnetization cease to evolve below T_g . This is also visible in Fig. 1, the open circles there becoming strictly horizontal below T_g . Bond rattling, on

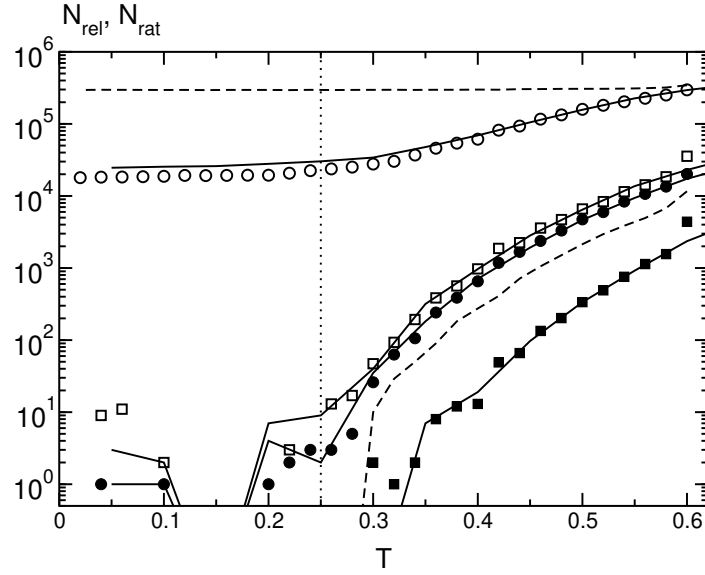


Figure 9: Number of accepted steps during equilibration of a large system. Symbols: slow cooling after quench to $T = 0.6$; circles: bond moves; squares: spin flips; filled: relaxation; empty: rattling. Full lines: same as symbols, but annealed. Dashed lines: spin moves with frozen bonds, upper: rattling, lower: relaxation. Vertical dotted line: T_g from Fig. 5.

the other hand, remains high and relatively constant throughout, in keeping with the analogy to ‘caged’ configurational movement.

This is in marked contrast to the behavior of a quenched-then-slowly-cooled system with random frozen bonds, shown by dashed lines. Spin moves in this case behave roughly as bond moves above. Relaxation stops above T_g , but spin rattling is remarkably constant down to lowest temperatures, as one would expect from the absence of a spin glass in 2D, *i.e.*, of an internal field to hold the spins in place. On the other hand, spin rattling in the 3D Edwards-Anderson model persists even below the spin-glass transition. This is in contrast to the 2D vitreous state, in which there are virtually no loose spins at all (Fig. 2).

Finally, we compare the results of a standard annealing run, shown by full lines. They are in excellent quantitative agreement with the supercooled liquid/glass — despite the latter being by definition metastable, as it consists of higher-energy configurations. This is further illustration of the long-lived

nature of the metastable ‘quasi’ equilibrium. In the absence of frustration, the difference in energy would translate into a larger number of accepted steps in the metastable case. This is actually observed at $T = 0.6$, but only because the system is quenched from $T = 5$ there. Even when shedding such a large energy, the excess steps are almost exclusively due to spins, indicating that the bond (‘configurational’) degree of freedom is most affected by frustration.

5 Discussion

The main problem with the identification of the glass in Section 3 is that χ_{SG} is not by itself a measure of frustration. It may function as such in a spin-glass setting, where one averages over many random bond configurations, so if two lattice copies ‘march in lockstep’ on the average, one can safely assume this is not due to the influence of the occasional ordered configuration.

Not so in our case, where the whole idea is that mobile bonds find rare configurations. In particular, they find the optimal amorphous ones, which show the same persistence of the initial divergence in χ_{SG} , as would a perfect ferromagnet. The glassy configurations are not far in energy (Fig. 1), so they, too, must contain large patches of the optimal arrangement.

The problem reduces to this: can one find a qualitative criterion to distinguish the ‘amorphous solid with defects’, the uppermost of the magnetization curves in Fig. 4, from the ‘supercooled liquid/glass’, the curve which forks down from it below T_0 ? Luckily, yes. It is provided by the field-dependence of χ_{SG} , shown in Figure 10 for the amorphous solid. The filled circles ($B = 0^+$) show the same behavior as in Figure 5, in line with the doubts expressed above. But the $B = 1$ curve (empty circles) is now entirely above the other one; in the annealed case, turning on the field increases χ_{SG} at all temperatures. The criterion follows, that if the field derivative of the spin-glass susceptibility

$$\left. \frac{\partial \chi_{SG}(T)}{\partial B} \right|_{B=0^+} \quad (7)$$

is positive at all temperatures, we have a solid. If it is negative around zero and changes sign at a finite $T = T_\ell$, we have a supercooled liquid.

This criterion makes physical sense. In the amorphous solid, the bonds are as good as frozen, since any rattling occurs in an optimally arranged background of spins and bonds. The spins opposing the field are in a minority

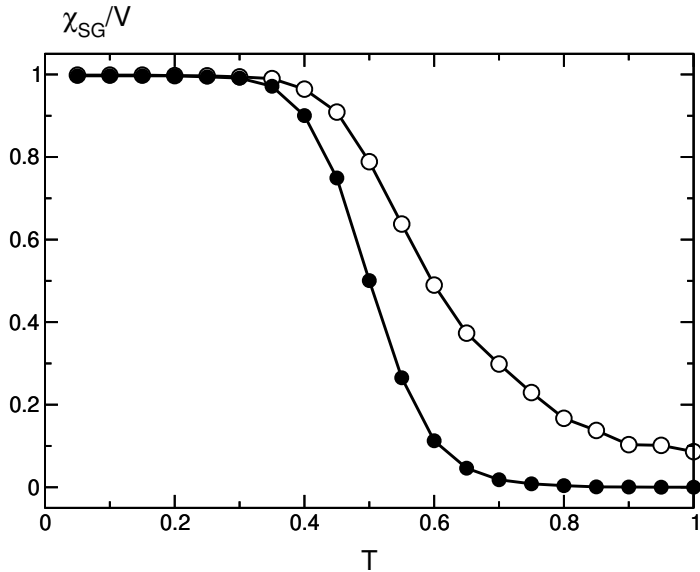


Figure 10: Same as Figure 5, but for the annealed state. Note the different field dependence.

(witness a finite magnetization), so increasing the field will make the system more rigid, increasing χ_{SG} at all temperatures.

Not so in the supercooled liquid, where the bonds rattle against a suboptimal background. At low temperatures, spin flips induced by the field will increase the range of bond movement, which in turn has a cascading influence (stochastic, of course) on spins in the bond path, degrading the correlation between the two copies of the lattice (see Fig. 8). At higher temperatures, however, there are already many spin flips, so this effect is ‘played out’; the spin majority orchestrated by the field then increases the correlation, like in the solid. The temperature at which the two tendencies balance is just T_ℓ .

This does not mean that T_ℓ is a thermodynamical (time-independent) temperature, indeed T_g itself is not, in any kinetic model. Given that it refers to the liquid state, T_ℓ is subject to the same time evolution as χ_{SG} in that regime, or the correlation function in Fig. 6. Nevertheless, the above argument implies that the appearance of a point, where the zero-field and finite-field susceptibilities cross, is generic for the supercooled liquid in this model, and will always be present for times between τ_β and τ_α . Since τ_β is so short, it can be observed without large numerical effort.

There are two things to note. First, the criterion for a supercooled bond

liquid implies (mildly) paradoxical behavior: the bonds ‘waiting to break out’ make the susceptibility *decrease* in response to an applied field, when $T < T_\ell$. The field has a net disorganizing effect on the spins, because it probes the configurational metastability of the supercooled liquid. Put simply, the uniform external field is in competition with the stochastic internal field, holding the spins in position for $T < T_\ell$.

Second, the glass itself is defined only quantitatively, as the manifold of states found on that part of the cooling curve of the supercooled liquid, where χ_{SG}/V saturates at unity. A qualitative characterization of T_g is not to be expected, on general grounds. In this context, the switch from circles to squares in Figure 5 may be interpreted, that if one takes a ‘snapshot’ of the system below T_ℓ at an arbitrary point in time, no analysis of that one snapshot can tell, whether it was taken above or below T_g .

It is easily shown that the maximally frustrated (vitreous) bond arrangements, found by the quenching algorithm, are a very small subset of all possible ones. For a state to be maximally frustrated, uncompensated bonds must be singletons, like in Fig. 2, each well separated from the others by a ‘layer’ of compensated ones, effectively ‘using up’ $q > 1$ bond positions for each singleton. Thus uncompensated bonds can choose only among some $2V/q$ positions, less than all $2V$ available ones. The number of distinct states is largest when the number of uncompensated bonds is one-half the total number of available positions, giving at most

$$\binom{2V/q}{V/q} \sim 4^{V/q} \quad (8)$$

states of this kind. On the other hand, supposing for simplicity that one has an equal number of positive and negative bonds ($p = 0.5$), the number of ways to place them on the lattice without restriction is

$$\binom{2V}{V} \sim 4^V, \quad (9)$$

of which the above q -th root is a vanishingly small fraction, when V is large. Energetically, the vitreous states are well separated from the bulk of the arbitrary ones, witness Fig. 1. They correspond to the ‘deep and narrow’ minima of glass theory. In fact, since their energy is determined by the number of singletons, Eq. 8 is also their degeneracy, ‘exponentially large’, as the general picture assumes. Since the algorithm is trapped in only one of

them in any given run (Fig. 6), one has ‘breaking of ergodicity’ [2] for times less than τ_α .

Let us summarize the analogies between our toy model and vitreous liquids. Bond and spin movement correspond to the configurational and orientational degrees of freedom, respectively. The diffusivity of bond movement reflects the absence of a kinetic energy contribution to the glass transition. The supercooled bond liquid turns into a glass if configurational rearrangements are artificially turned off. Spin disorder changes very little across the glass transition, but spin movement ceases there, as well as all relaxation. Configurational (bond) rattling persists to lowest temperatures. Somewhat above our original ambitions, the zero-field glass transition in the model occurs at about one-third the melting temperature, $T_g \approx T_0/3$, an old rule of thumb in glass formers [1].

6 Conclusion

We have realized a spin glass in the two-dimensional bond-disordered Ising model on a square lattice, by taking into account only a small subset of impurity arrangements. This subset was generated by a quenching algorithm which imitated vitrification in liquids, by allowing diffusion of impurity bonds over the lattice. The crossover between the glassy and high-temperature (melted) state was identified as a supercooled liquid. To distinguish from customary usage of the term ‘spin glass’, and to emphasize our glass is kinetic, not thermodynamic, we propose the terms ‘bond glass’ and ‘supercooled bond liquid’, respectively. A macroscopic criterion was shown to distinguish the supercooled liquid from the amorphous solid, connected to the ground-state manifold by slow cooling, which is this model’s analogue of the crystal state of vitreous liquids. The criterion provides an opportunity to study field and temperature hysteretic effects on the formation of the supercooled bond liquid.

7 Acknowledgements

Conversations with K. Uzelac and S. Barišić, and one with M. Mézard, are gratefully acknowledged. This work was supported by the Croatian Government under Project 119 204.

References

- [1] W. Kauzmann, Chem. Rev. **43** (1948) 219.
- [2] C.A. Angell, Science **267** (1995) 1924.
- [3] K. Binder, Rev. Mod. Phys. **58** (1986) 802.
- [4] A.P. Young, J.D. Reger and K. Binder, in *The Monte Carlo Method in Condensed Matter Physics*, K. Binder, ed., Topics in Applied Physics, vol. 71, Springer 1995, p. 355.
- [5] G. Toulouse, Commun. Phys. **2** (1977) 115.
- [6] R.N. Bhatt and A.P. Young, Phys. Rev. B **37** (1988) 5606.
- [7] G.H. Frederickson and H.C. Andersen, Phys. Rev. Lett. **53** (1984) 1244.
- [8] A. Coniglio, Prog. Th. Phys. Suppl. **126** (1997) 281.
- [9] V. Cataudella, G. Franzese, M. Nicodemi, A. Scala, and A. Coniglio, Phys. Rev. E **54** (1996) 175.
- [10] R. Schmitz, J.W. Dufty, P. De, Phys. Rev. Lett. **71** (1993) 2066.
- [11] E.E. Vogel, S. Contreras, M.A. Osorio, J. Cartes, F. Nieto, and A.J. Ramírez-Pastor, Phys. Rev. B **58** (1998) 8475.
- [12] S.F. Edwards and P.W. Anderson, J. Phys. F. **5** (1975) 965.
- [13] J. Kisker, L. Santen, M. Schreckenberg, and H. Rieger, Phys. Rev. B **53** (1996) 6418.